Polyanthraquinone as a Reliable Organic Electrode for Stable and Fast Lithium Storage

Zhiping Song, Yumin Qian, Mikhail L. Gordin, Duihai Tang, Terrence Xu, Minoru Otani, Hui Zhan, Haoshen Zhou,* and Donghai Wang*

Abstract: *In spite of recent progress, there is still a lack of reliable organic electrodes for Li storage with high comprehensive performance, especially in terms of long-term cycling stability. Herein, we report an ideal polymer electrode based on anthraquinone, namely, polyanthraquinone (PAQ), or specifically, poly(1,4-anthraquinone) (P14AQ) and poly(1,5-anthraquinone) (P15AQ). As a lithium-storage cathode, P14AQ showed exceptional performance, including reversible capacity almost equal to the theoretical value (260 mA h g^{-1}; > 257 mA h g^{-1} for AQ), a very small voltage gap between the charge and discharge curves (2.18–2.14 = 0.04 V), stable cycling performance (99.4 % capacity retention after 1000 cycles), and fast-discharge/charge ability (release of 69 % of the low-rate capacity or 64 % of the energy in just 2 min). Exploration of the structure–performance relationship between P14AQ and related materials also provided us with deeper understanding for the design of organic electrodes.*

Although state-of-the-art lithium-ion batteries have penetrated into all aspects of our society, their development still lags behind our demands for energy-storage devices, not just in terms of their charge/discharge performance, but also their safety, cost, sustainability, and environmental friendliness.[1] Therefore, many scientists have shifted their attention to new battery types, such as sodium-ion, lithium–sulfur, and lithium-

air batteries. Organic electrode materials have also attracted increasing attention in recent years owing to their promising electrochemical performance and distinct advantages in sustainability and environmental friendliness.[2,3] Additionally, the unique features of organic materials, such as structure diversity, solubility, flexibility, and processability, make them promising candidates for cathodes or anodes of various energy-storage devices,[3] including rechargeable Li,[4–10] Na,[8,11–13] and Mg batteries,[14] supercapacitors,[15] thin-film batteries,[16] aqueous rechargeable batteries,[17,18] redox flow batteries,[19] and even all-organic batteries.[13,19,20]

Organic materials based on conjugated carbonyl compounds,[21] especially quinones, are believed to be among the most promising types of organic lithium-storage electrodes owing to their high theoretical capacity (up to 600 mA h g^{-1}),[4] high redox reversibility, and high resource availability. For quinone-based materials, the commercial small organic molecules, such as benzoquinone (BQ),[22–24] naphthoquinone (NQ), anthraquinone (AQ)[6,25,26] (Figure 1a), and their derivatives, can not be used directly in

[*] Dr. Z. Song, Dr. M. L. Gordin, Dr. D. Tang, Dr. T. Xu, Prof. D. Wang
Department of Mechanical and Nuclear Engineering
The Pennsylvania State University, University Park, PA 16802 (USA)
E-mail: dwang@psu.edu

Dr. Z. Song, Dr. Y. Qian, Prof. H. Zhou
Research Institute for Energy Conservation
National Institute of Advanced Industrial Science and Technology
Tsukuba, Ibaraki 305-8568 (Japan)
E-mail: hs.zhou@aist.go.jp

Dr. Z. Song, Prof. H. Zhan
Department of Chemistry, Wuhan University
Wuhan 430072 (China)

Prof. M. Otani
Nanomaterials Research Institute
National Institute of Advanced Industrial Science and Technology
Tsukuba, Ibaraki 305-8568 (Japan)
and
Elements Strategy Initiative for Catalysts and Batteries
Kyoto University, Katsura, Kyoto 615-8520 (Japan)

Prof. H. Zhou
National Laboratory of Solid State Microstructures
Department of Energy Science and Engineering
Nanjing University, Nanjing 210093 (China)

Supporting information for this article is available on the WWW under http://dx.doi.org/10.1002/anie.201506673.
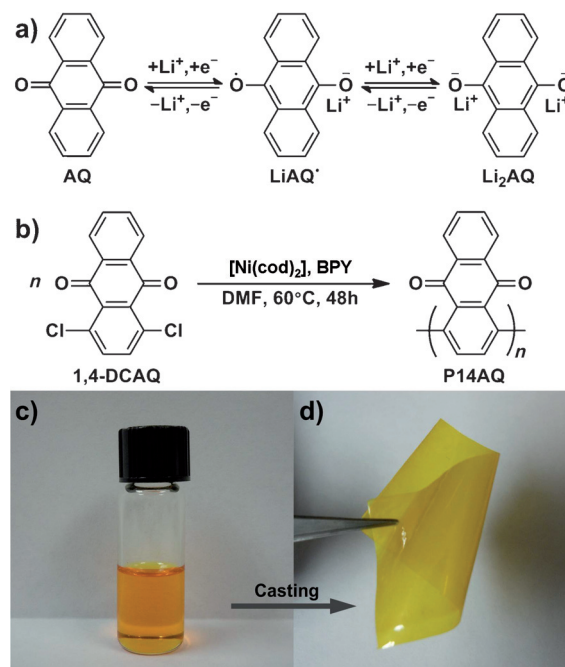
Figure 1. a) Electrochemical redox mechanism of the AQ unit. b) Synthetic route to P14AQ. c) Photograph of a solution of P14AQ in chloroform (10 g L^{-1}). d) Photograph of a free-standing and flexible P14AQ thin film (3 × 2 cm²) cast from the solution. BPY = 2,2'-bipyridine, cod = 1,5-cyclooctadiene, DMF = N,N-dimethylformamide.

common rechargeable Li batteries with non-aqueous electrolytes. Under these conditions, the active materials (including their discharged forms) dissolve to a significant extent, which decreases their discharge/charge stability and results in poor cycle life. This problem can be alleviated—though not solved—by enhancing the immobilization of active materials (e.g., by the formation of composites with carbon nanotubes[25] or mesoporous carbon[26]), or by using lithium-ion-selective separators (e.g., LISICON[23] or PEO[24]) to prevent the dissolved molecules and/or anions from migrating to the anode side. However, these methods still result in unsatisfactory long-term cycling performance. Thus, the most reliable approach is to develop inherently insoluble compounds containing dense quinone groups to simultaneously satisfy the requirements for energy density and cycle life. In the past few years, some successful examples were reported, including organic polymers (e.g., PBQS[8] and PPYT[9]), organic salts (e.g., $Li_4C_8H_2O_6$[20]), and oligomeric salts (e.g., $Li_2PDHBQS$[7]). These materials show cycling stability comparable to that of inorganic layered oxides (for example, $Li_2PDHBQS$ retains 90% of its reversible capacity after 1500 cycles[7]), but still lag far behind zero-strain inorganic materials (e.g., $LiFePO_4$ and $Li_4Ti_5O_{12}$) with negligible capacity fading during hundreds of cycles.

Our strategy is to develop quinone-based polymers with simple structures and an uncomplicated synthesis. To construct a polymer, the monomeric units can be linked by various organic groups, such as methylene ($-CH_2-$),[10] imine ($-NH-$),[27] ether ($-O-$), and thioether groups ($-S-$),[6–8] or just grafted on a skeleton chain.[9,17] These approaches will lead to a decrease in theoretical capacity to varying degrees because of the addition of inactive moieties. Ideally, the electroactive rings should be coupled directly without any linker. This approach would slightly increase the theoretical capacity and may facilitate electron transport along the chain because of enhanced structural conjugation. We found that anthraquinone (AQ) rings can be coupled to form polyanthraquinone (PAQ)[28] through a one-step condensation polymerization reaction (Figure 1b).[29] By using 1,4-dichloro-anthraquinone (1,4-DCAQ) or 1,5-dichloroanthraquinone (1,5-DCAQ) as the monomer, we successfully synthesized poly(1,4-anthraquinone) (P14AQ) and poly(1,5-anthraquinone) (P15AQ), respectively, which we then applied as cathodes for rechargeable Li batteries. Both PAQs showed high electroactivity, and, to our surprise, P14AQ showed exceptional comprehensive performance, superior to that of all previously reported organic electrodes, including the absence of capacity decay during 1000 discharge/charge cycles.

Both PAQs were synthesized mainly according to a previously reported procedure[29] and characterized by various methods, including elemental analysis, FTIR and NMR spectroscopy, XRD, SEM, and thermogravimetric analysis (see the Supporting Information for detailed procedures and analysis, including Figures S1–S3). Unlike P15AQ and previous polymer electrode materials, which are insoluble in common organic solvents, P14AQ is very soluble in chloroform. Moreover, the resulting transparent yellow solution (Figure 1c) can be readily cast to form a free-standing and

flexible thin film (Figure 1d). These unique properties open up tremendous potential for the application of P14AQ in many novel battery designs, such as flexible thin-film batteries, printed batteries, and even transparent batteries.

The structure–performance relationship between a monomer and polymers derived from the monomer by different linking methods is important for the design of high-performance polymer electrode materials, but is rarely investigated. We semiquantitatively studied this relationship by theoretical calculations and electrochemical tests for the AQ monomer, poly(anthraquinonyl sulfide) (PAQS),[6] P14AQ, and P15AQ. It is well-known that the energy level of the lowest unoccupied molecular orbital (LUMO) of an n-type electroactive material is a useful parameter for estimating its relative redox potential (a lower LUMO energy level corresponds to a higher reduction potential).[7–9,30] We used the optimized geometries of AQ, PAQS, P14AQ, and P15AQ (see Figure S4 in the Supporting Information) to calculate their electron configurations (Figure 2a) by a method based on density functional theory (DFT). The polymers were modeled as short chains containing five structural units to keep the calculations manageable; this approach has already been shown to be simple but effective.[8] For the AQ monomer, the LUMO energy level is located at −2.80 eV (consistent with the previously reported value[30]), and the experimental discharge plateau is rather flat at 2.26 V versus Li^+/Li (Figure 2b), thus indicating a two-phase redox reaction between AQ and Li_2AQ. In contrast, each polymer has five nearly degenerate orbitals located nearby (the lower/upper values are −3.01/−2.54, −2.72/−2.59, and −2.72/−2.55 eV for PAQS, P14AQ, and P15AQ, respectively), and the electron configurations of P14AQ and P15AQ are very similar. Assuming that the electron configurations are rigid, electrons will successively fill the unoccupied orbitals from the lowest- to the highest-energy orbital during the reduction process, thus leading to the experimentally observed sloping discharge curves of the polymers (Figure 2b). The slopes for P14AQ and P15AQ are much smaller than that for PAQS since their characteristic energy levels are more intensive (the band widths are 0.47, 0.13, and 0.17 eV for PAQS, P14AQ, and P15AQ, respectively). The average discharge voltages of AQ, PAQS, P14AQ, and P15AQ are 2.24, 2.14, 2.14, and 2.09 V versus Li^+/Li, respectively, thus mimicking the trend in the relative position of the center of the energy-level band (−2.80, −2.78, −2.65, and −2.63 eV for AQ, PAQS, P14AQ, and P15AQ, respectively). This trend is also reflected in the cyclic voltammetry (CV) curves (see Figure S5), in which the peak widths of P14AQ and P15AQ are much narrower than that of PAQS; the cathodic peak voltages also approximately follow this trend. Thus, the difference in the electrochemical behavior of AQ and its polymers, despite their identical redox mechanism (Figure 1a), is well explained by the DFT calculations.

The theoretical capacities calculated from the two-electron redox reaction of the AQ unit (Figure 1a) are 257, 225, 260, and 260 mA h g^{-1} for AQ, PAQS, P14AQ, and P15AQ, respectively (Figure 2a). These values were used to define the current rate (mA g^{-1}) of 1 C for each material. At 0.2 C, the number of electrons delivered per unit is close to 2 for each
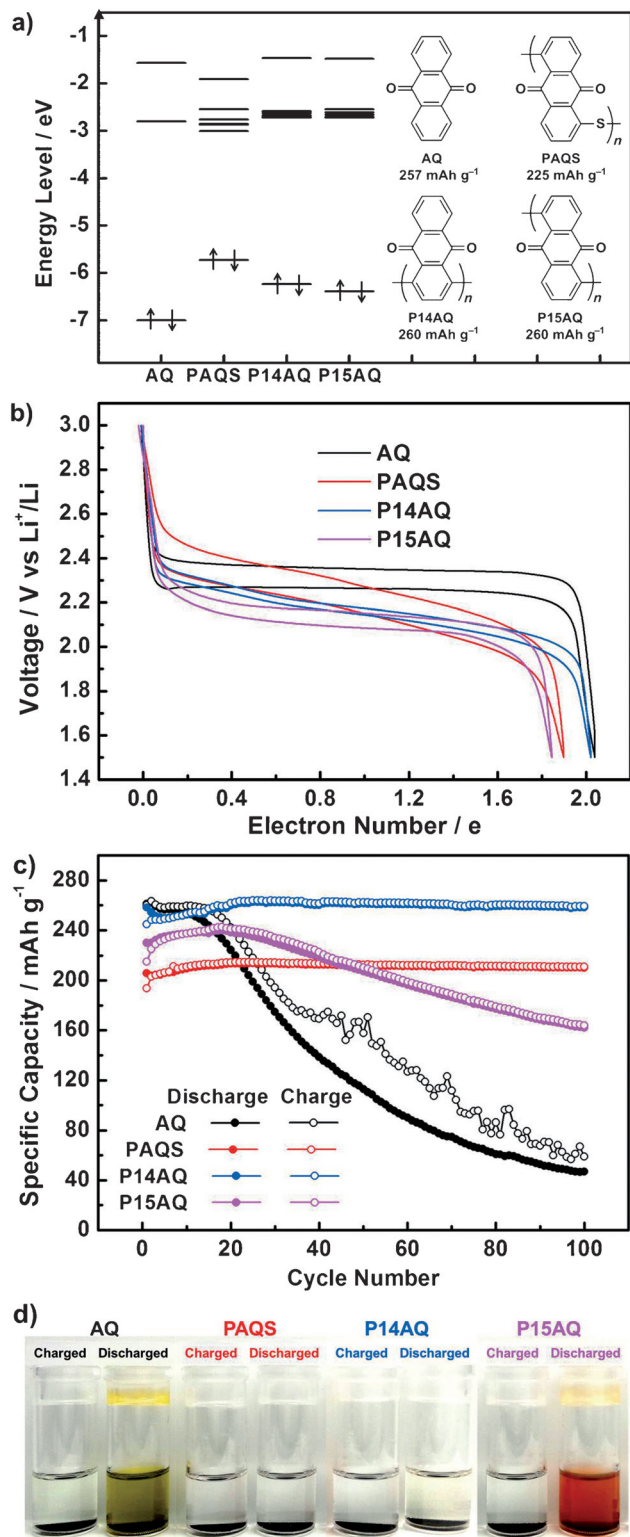
Figure 2. Comparison of the four materials AQ, PAQS, P14AQ, and P15AQ. a) Structure and theoretical capacity of the materials, and the electron configuration obtained by DFT calculations. b) Typical voltage profiles at a current rate of 0.2 C. c) Cycling profiles at a current rate of 0.2 C, with a cutoff voltage of 1.5–3.0 V. d) Photographs showing the dissolution behavior of the materials. In each vial, the electrode film in the charged state (as-fabricated) or discharged state (discharged to 1.5 V) was immersed in 1 mL of the electrolyte (1 M LiTFSI/DOL+DME, 2:1, v/v) for 24 h. LiTFSI = lithium bis(trifluoromethanesulfonyl)imide, DOL = 1,3-dioxolane, DME = 1,2-dimethoxyethane.

material (2.04, 1.90, 2.02, and 1.85 for AQ, PAQS, P14AQ, and P15AQ, respectively; Figure 2b), thus indicating the full utilization of AQ units for all materials. However, the cycling performance of AQ and P15AQ leaves much to be desired. The discharge capacity retention at the 100th cycle was 17.8, 98.4, 98.3, and 67.6%, for AQ, PAQS, P14AQ, and P15AQ, respectively (Figure 2c). It is easy to understand why the AQ monomer showed the worst cycling stability from the serious dissolution of its discharged form (Li$_2$AQ) in the electrolyte (Figure 2d). Of the polymers, only discharged P15AQ showed similar dissolution behavior, mainly caused by the relatively low molecular weight of the polymer (ca. 230000 for P14AQ and ca. 2300 for P15AQ, as estimated from the C/Cl molar ratio; see the Supporting Information). The higher solubility of the discharged phases of these materials stands in contrast to the behavior of our previously studied 2,5-dihydroxy-*p*-benzoquinone-based materials, the discharged phases of which were less soluble because of enhanced O···Li···O coordination bonds.[7] As the AQ-based materials probably have less C=O and C−O bonds but larger steric hindrance, the O···Li···O coordination bonds formed in the discharged product are not strong enough to offset the enhanced negative-charge repulsion between monomeric AQ rings or short polymer chains. The different dissolution behavior of the four materials agrees well with their different cycling performance, thus leading us to believe that the unfavorable dissolution is the dominating factor in capacity fading.

From the above comparisons, we can see that P14AQ shows the best electrochemical performance of the four materials, in terms of both discharge capacity and cycling stability. The energy density was calculated to be 560 W h kg^{-1} (2.14 V × 263 mA h g^{-1}), which is actually slightly higher than that of LiCoO$_2$ (3.8 V × 140 mA h g^{-1} = 530 W h kg^{-1}). The high-rate and long-term cycling performance of P14AQ was further studied under various test conditions (Figure 3). Relative to the maximum capacity of 263 mA h g^{-1} at 0.2 C, the capacity retention was 98, 96, 91, 84, 78, and 69% at increased current rates of 0.5, 1, 2, 5, 10, and 20 C, respectively (Figure 3a). P15AQ also revealed similar rate capability if the capacity decay caused by dissolution is taken into account, thus indicating that its electrolchemical performance could be improved to a level similar to that of P14AQ by increasing the molecular weight of the polymer. Little electrochemical polarization was observed in the corresponding voltage profiles of P14AQ (Figure 3b); the average discharge voltage was 1.97 V even at 20 C (the value is 2.14 V at 0.2 C). A large capacity of 182 mA h g^{-1}, corresponding to a large energy density of approximately 360 W h kg^{-1}, was thus attained in nearly 2 min. This high-rate performance is superior to most other reported results for pristine organic or inorganic electrodes. Figure 3c shows the long-term cycling performance of P14AQ at moderate current rates of 1 and 2 C. The reversible capacity reached 248 and 235 mA h g^{-1}, respectively, after the initial several cycles of activation, and then remained very stable for 1000 cycles: The capacity retention was 98.1 and 99.4% after 1000 cycles at 1 and 2 C, respectively. Moreover, the Coulombic efficiency stabilized above 99.8% at 1 C or 99.9% at 2 C after the first few cycles. To the best of our knowledge, on the basis of the above data,
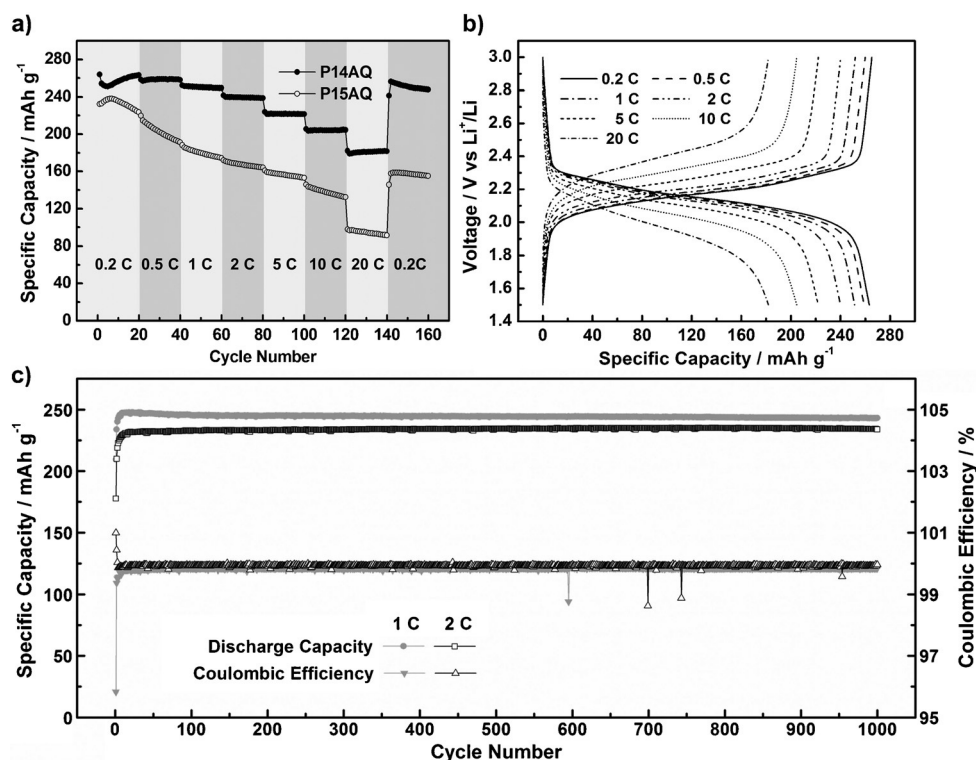
Figure 3. a) Discharge-capacity profiles versus cycle number for P14AQ and P15AQ at a changing current rate (from 0.2 to 20 C). b) Corresponding voltage profiles of P14AQ at different current rates. c) Long-term cycling profiles (1000 cycles) of P14AQ at a current rate of 1 or 2 C.

calculations and dissolution-behavior tests, respectively. Further electrochemical measurements showed the excellent fast-discharge/charge ability (20 C, 69%) and long-term cycling stability (1000 cycles, 99.4%) of P14AQ, which takes the battery performance of organic electrode materials to a new level. The exceptional battery performance of P14AQ, in addition to its convenient solubility in chloroform and good film-forming ability, offer tremendous potential for applications in the next generation of high-performance, sustainable, green, and flexible energy-storage devices.

Acknowledgements

P14AQ shows the highest cycling stability among reported organic electrodes, and is even comparable to zero-strain inorganic electrodes, such as LiFePO$_4$ and Li$_4$Ti$_5$O$_{12}$.

To find out why P14AQ shows such superior electrochemical performance, we measured its CV curves at different scan rates and carried out electrochemical impedance spectroscopy (EIS) of P14AQ in different states (see Figure S7 and detailed analysis in the Supporting Information). We ascribe the fast-discharge/charge ability to the high redox reversibility of P14AQ (the charge/discharge voltage gap is only 0.04 V in Figure 2b) as a result of the surface reaction (verified by the linear relationship between peak current and scan rate; see Figure S7a) of the amorphous quinone polymer. For the long-term cycling stability, the absolute insolubility (Figure 2d) is an important prerequisite, and the small change in charge-transfer resistance (R_{CT}) during 200 cycles (see Figure S7b and Table S1) also indicates the stable microstructure of the P14AQ electrode, probably as a result of the amorphous morphology (see Figure S2), high molecular weight, and high purity of the polymer.

In summary, we have developed a novel type of polymer electrode material: polyanthraquinone. P14AQ and P15AQ both showed high redox reversibility as cathodes for rechargeable Li batteries, with high energy density comparable to that of LiCoO$_2$ (2.14 V × 263 mAh g^{-1} = 563 Wh kg^{-1} for P14AQ and 2.09 V × 240 mAh g^{-1} = 502 Wh kg^{-1} for P15AQ). The differences in the discharge curves and cycling performance of AQ, PAQS, P14AQ, and P15AQ are explained well by DFT

[1] D. Larcher, J.-M. Tarascon, *Nat. Chem.* **2015**, *7*, 19–29.
[2] Y. Liang, Z. Tao, J. Chen, *Adv. Energy Mater.* **2012**, *2*, 742–769.
[3] Z. Song, H. Zhou, *Energy Environ. Sci.* **2013**, *6*, 2280–2301.
[4] H. Chen, M. Armand, G. Demailly, F. Dolhem, P. Poizot, J.-M. Tarascon, *ChemSusChem* **2008**, *1*, 348–355.
[5] M. Armand, S. Grugeon, H. Vezin, S. Laruelle, P. Ribière, P. Poizot, J.-M. Tarascon, *Nat. Mater.* **2009**, *8*, 120–125.
[6] Z. Song, H. Zhan, Y. Zhou, *Chem. Commun.* **2009**, 448–450.
[7] Z. Song, Y. Qian, X. Liu, T. Zhang, Y. Zhu, M. Otani, H. Zhou, *Energy Environ. Sci.* **2014**, *7*, 4077–4086.
[8] Z. Song, Y. Qian, T. Zhang, M. Otani, H. Zhou, *Adv. Sci.* **2015**, 1500124.
[9] T. Nokami, T. Matsuo, Y. Inatomi, N. Hojo, T. Tsukagoshi, H. Yoshizawa, A. Shimizu, H. Kuramoto, K. Komae, H. Tsuyama, J.-i. Yoshida, *J. Am. Chem. Soc.* **2012**, *134*, 19694–19700.
[10] W. Huang, Z. Zhu, L. Wang, S. Wang, H. Li, Z. Tao, J. Shi, L. Guan, J. Chen, *Angew. Chem. Int. Ed.* **2013**, *52*, 9162–9166; *Angew. Chem.* **2013**, *125*, 9332–9336.
[11] L. Zhao, J. Zhao, Y.-S. Hu, H. Li, Z. Zhou, M. Armand, L. Chen, *Adv. Energy Mater.* **2012**, *2*, 962–965.
[12] H.-g. Wang, S. Yuan, D.-l. Ma, X.-l. Huang, F.-l. Meng, X.-b. Zhang, *Adv. Energy Mater.* **2014**, *4*, 1301651.

[13] S. Wang, L. Wang, Z. Zhu, Z. Hu, Q. Zhao, J. Chen, *Angew. Chem. Int. Ed.* **2014**, *53*, 5892 – 5896; *Angew. Chem.* **2014**, *126*, 6002 – 6006.

[14] H. Sano, H. Senoh, M. Yao, H. Sakaebe, T. Kiyobayashi, *Chem. Lett.* **2012**, *41*, 1594 – 1596.

[15] G. A. Snook, P. Kao, A. S. Best, *J. Power Sources* **2011**, *196*, 1 – 12.

[16] H. Wu, S. A. Shevlin, Q. Meng, W. Guo, Y. Meng, K. Lu, Z. Wei, Z. Guo, *Adv. Mater.* **2014**, *26*, 3338 – 3343.

[17] W. Choi, D. Harada, K. Oyaizu, H. Nishide, *J. Am. Chem. Soc.* **2011**, *133*, 19839 – 19843.

[18] H. Qin, Z. P. Song, H. Zhan, Y. H. Zhou, *J. Power Sources* **2014**, *249*, 367 – 372.

[19] F. R. Brushett, J. T. Vaughey, A. N. Jansen, *Adv. Energy Mater.* **2012**, *2*, 1390 – 1396.

[20] S. Wang, L. Wang, K. Zhang, Z. Zhu, Z. Tao, J. Chen, *Nano Lett.* **2013**, *13*, 4404 – 4409.

[21] B. Häupler, A. Wild, U. S. Schubert, *Adv. Energy Mater.* **2015**, *5*, 1402034.

[22] M. Yao, H. Senoh, S.-i. Yamazaki, Z. Siroma, T. Sakai, K. Yasuda, *J. Power Sources* **2010**, *195*, 8336 – 8340.

[23] H. Senoh, M. Yao, H. Sakaebe, K. Yasuda, Z. Siroma, *Electrochim. Acta* **2011**, *56*, 10145 – 10150.

[24] Y. Hanyu, Y. Ganbe, I. Honma, *J. Power Sources* **2013**, *221*, 186 – 190.

[25] M. Lee, J. Hong, H. Kim, H.-D. Lim, S. B. Cho, K. Kang, C. B. Park, *Adv. Mater.* **2014**, *26*, 2558 – 2565.

[26] K. Zhang, C. Guo, Q. Zhao, Z. Niu, J. Chen, *Adv. Sci.* **2015**, *2*, 1500018.

[27] A. Vlad, K. Arnould, B. Ernould, L. Sieuw, J. Rolland, J.-F. Gohy, *J. Mater. Chem. A* **2015**, *3*, 11189 – 11193.

[28] Y. Zhou, B. Wang, C. Liu, N. Han, X. Xu, F. Zhao, J. Fan, Y. Li, *Nano Energy* **2015**, *15*, 654 – 661.

[29] T. Yamamoto, H. Etori, *Macromolecules* **1995**, *28*, 3371 – 3379.

[30] M. Yao, S.-i. Yamazaki, H. Senoh, T. Sakai, T. Kiyobayashi, *Mater. Sci. Eng. B* **2012**, *177*, 483 – 487.